Ionics (2015) 21:1731–1740
DOI 10.1007/s11581-014-1339-1

ORIGINAL PAPER

A glassy carbon electrode modified with MCM-41/nickel hydroxide nanoparticle/multiwalled carbon nanotube composite as a sensor for the simultaneous determination of dopamine, piroxicam, and cefixime

Ali Babaei · Mohammad Afrasiabi

Received: 15 June 2014 / Revised: 22 November 2014 / Accepted: 2 December 2014 / Published online: 9 January 2015

Abstract The present work demonstrates that simultaneous determination of dopamine (DA), piroxicam (PRX), and cefixime (CEF) can be performed on the composite of multiwalled carbon nanotubes (MWCNTs), nickel hydroxide nanoparticles (NHNPs), and MCM-41 modified glassy carbon electrode (MWCNTs-NHNPs-MCM-41/GCE). The effect of the composition of MWCNTs, NHNPs, and MCM-41 for the modification of GCE was tested, and the mixture of 5 % NHNPs, 10 % MCM-41, and 85 % MWCNTs was chosen for the fabrication of the sensor. The MWCNTs-NHNPs-MCM-41 composite was characterized by Fourier transform infrared (FTIR), scanning electron microscopy (SEM), and energy-dispersive X-ray (EDX) analysis. Under optimum conditions, the application of differential pulse voltammetry method showed the linear relationship between oxidation peak currents, and the corresponding concentrations of DA, PRX, and CEF were 0.2–85, 0.1–70, and 0.1–200 μM with detection limits of 0.07, 0.04, and 0.05 μM, respectively. The proposed method was used in the determination of these compounds in human urine and blood serum samples with satisfactory results.

Keywords Dopamine · Piroxicam · Cefixime · Electrochemical sensor · Modified electrode

Electronic supplementary material The online version of this article (doi:10.1007/s11581-014-1339-1) contains supplementary material, which is available to authorized users.

A. Babaei (✉) · M. Afrasiabi
Department of Chemistry, Faculty of Science, Arak University, ArakP.O. Box 38156-8-8349, Iran
e-mail: ali.babaei08@gmail.com

A. Babaei
Research Center for Nanotechnology, Arak University, ArakP.O. Box 38156-8-8349, Iran

Introduction

Carbon nanotubes (CNTs) have attracted much attention due to their structural uniqueness, chemical and physical properties, and potential applications [1]. The subtle electronic behavior of CNTs reveals that they have the ability to mediate electron transfer reactions of electroactive species in solution when they are used as the electrode modifier.

Transition-metal nanoparticles in different forms have emerged as a family of catalysts able to promote more efficiently a variety of organic transformations because of their small size and extremely large surface-to-volume ratio [2, 3]. Nickel hydroxide nanoparticles (NHNPs) with a small crystalline size show excellent electrochemical performance. Many precipitation methods for preparing NHNPs have been reported [4–6]. Among those methods, the method of coordination homogeneous precipitation is new and facile, needing no expensive raw materials or equipment, is also easy for mass production, and can be extended to synthesize other hydroxide or oxide nanocrystals. Therefore, in this work, we used the coordination homogeneous precipitation method for the synthesis of NHNPs.

MCM-41 was the first synthetic mesoporous material and one member of the mesoporous molecular sieves of the M41S family with regularly ordered pore arrangement and a very narrow pore distribution, which was disclosed by the Mobil scientists in 1992 [7]. MCM-41 can act as a catalyst, catalyst support [8], or as a host for host-guest nanocomposite materials [9]. It has also been applied as an adsorbent material [10] and as a material for electrochemiluminescence [11] and electrochemical sensors [12, 13]. This is mainly because MCM-41 can offer a large surface area, controllable pore size, high porosity, ordered uniform pore structure, and high loading capacity. It is a strong Lewis acid and, therefore, has been used for catalysis purposes in organic synthesis reactions. It means that substances with strong base properties have a

strong interaction with MCM-41. These unique properties of MCM-41 lead us to use it as a modifier of the proposed sensor.

There is considerable interest in developing studies of neurotransmitters such as dopamine (DA). DA is a ubiquitous neurotransmitter in mammalian brain tissues that plays an important physiological role in the functioning of the central nervous, renal, hormonal, and cardiovascular systems as an extracellular chemical messenger [14]. DA belongs to the family of inhibitory neurotransmitters; its function is to regulate neural interactions by reducing permeability of gap junctions between adjacent neurons of the same type. Variation of DA concentration in the body is also involved in neurological diseases such as Parkinson's and Alzheimer's disease [15].

Piroxicam (or 4-hydroxy-2-methyl-N-2-pyridinyl-2H-1,2-benzothiazine-3-carboxamide 1,1-dioxide or feldene—PRX) is a nonsteroidal anti-inflammatory drug that also possesses analgesic and antipyretic properties. This drug has been widely used in the treatment of rheumatoid arthritis and other inflammatory disorders [16]. A number of methods including high-performance liquid chromatography, double-beam UV spectrophotometry, spectrofluorometry [17], thin layer chromatography [18], and voltammetric methods [5] were reported for the determination of PRX.

Cefixime (CEF) is a cephalosporin antibacterial that inhibits bacterial cell wall synthesis. Cephalosporins are semisynthetic antibacterial agent derived from cephalosporin C. Reviewing the literature revealed that several methods have been used for the determination of CEF in pure form, pharmaceutical formulations, or in biological samples, whether as a single active ingredient or in combination with other drugs, and these methods include high-performance liquid chromatography [19], high-performance thin layer chromatography [20], and spectrofluorimetric [21] and voltammetric methods [22, 23].

CEF is a third-generation cephalosporin drug, of which its high consumption could lead to renal tubular necrosis. The side effect of a high usage of PRX is damage of a kidney. These two compounds might be prescribed as combined medicines during sickness like cold and flu. In addition, a high dosage of DA could also increase the levels of urea in a body which accelerates the side effects of these medicines [24]. Therefore, simultaneous determinations of CEF, PRX, and DA might be interesting. As far as our knowledge is concerned, there is no report on the electrochemical simultaneous determination of DA, PRX, and CEF compounds. For these reasons, developing an electrochemical method for the simultaneous determination of DA, PRX, and CEF would be of great value. The linear dynamic range and detection limit of the proposed method were compared with other reported electrochemical methods for the determination of DA, PRX, and CEF (Table 1).

Experimental

Reagents and solutions

All chemicals were of analytical grade and used without further purification. DA, PRX, and CEF were obtained from Acros, Sigma, and Merck chemical companies, respectively. Multiwalled carbon nanotubes (MWCNTs; >95 wt%, 5–20 nm) were purchased from PlasmaChem GmbH Company.

Table 1 Comparison of merits of voltammetry methods for determination of DA, PRX, and CEF

Analyte	Electrode	Linear dynamic range (μM)	Detection limit (μM)	Reference
DA	Palladium nanoparticle-loaded carbon nanofibers/carbon paste electrode	0.5–160	0.2	[25]
	Mixed ruthenium oxide hexacyanoferrate/ruthenium hexacyanoferrate/glassy carbon electrode	0.50–10 and 25–550	0.195	[26]
	Thin pyrolytic carbon films	18–270	2.3	[27]
	Carboxylated carbonaceous spheres/glassy carbon electrodes	0.1–40	0.03	[28]
	Overoxidized polypyrrole/grapheme/glassy carbon electrode	0.50–10 and 25–1000	0.1	[29]
	Multiwalled carbon nanotubes/nickel hydroxide nanoparticles/MCM-41/glassy carbon electrode	0.2–85	0.07	This work
PRX	Chitosan-doped carbon nanoparticles/plain pyrolytic graphite electrode	0.05–50	0.025	[30]
	Nickel hydroxide nanoparticles/multiwalled carbon nanotubes/glassy carbon electrode	0.7–75	0.11	[5]
	Multiwalled carbon nanotubes/carbon paste electrode	0.15–5	0.1	[31]
	Multiwalled carbon nanotubes/nickel hydroxide nanoparticles/MCM-41/glassy carbon electrode	0.1–70	0.04	This work
CEF	Hanging mercury drop electrode	0.06–12	0.046	[32]
	Multiwalled carbon nanotubes decorated with $NiFe_2O_4$ magnetic nanoparticles	0.1–100 and 100–600	0.02	[22]
	Gold nanoparticles electrodeposited on a multiwalled/carbon paste electrode	0.01–200	0.003	[23]
	Multiwalled carbon nanotubes/nickel hydroxide nanoparticles/MCM-41/glassy carbon electrode	0.1–200	0.05	This work

Stock standard solutions of 10 mM DA, 10 mM PRX, and 10 mM CEF were freshly prepared in 0.1 M phosphate buffers of pH=5. All other DA, PRX, and CEF solutions were prepared by diluting the stock standard solutions using 0.1 M phosphate buffer (pH=5). Phosphate buffer solutions (PBS) were prepared from the stock solution of 0.1 M KH_2PO_4 and 0.1 M K_2HPO_4. pH was adjusted using concentrated H_3PO_4 or NaOH solutions. Electrochemical experiments on DA, PRX, and CEF were carried out in 0.1 M PBS at pH 5. Fresh human serum samples were obtained from Razi Institute of Vaccine and Serum Company (Tehran, Iran). The human serum and urine samples were filtered and diluted 50 times using 0.1 M PBS)pH=5(and used for the determination of the recovery by spiking with DA, PRX, and CEF compounds.

Instrumentation

All voltammetric measurements were carried out using MWCNTs-NHNPs-MCM-41/GCE as the working electrode, an Ag/AgCl/3 M KCl electrode as the reference electrode, and a platinum wire as an auxiliary electrode. Differential pulse voltammetry (DPV), cyclic voltammetry (CV), and electrochemical impedance spectroscopy (EIS) experiments were carried out using an Autolab PGSTAT 30 potentiostat galvanostat (EcoChemie, The Netherlands) coupled with a 663 VA stand (Metrohm, Switzerland). All potentials given are with respect to the potential of the reference electrode. The pH measurements were performed with a Metrohm 744 pH meter using a combination glass electrode. The morphological analyses were carried out using Sigma VP Zeiss SEM instrument. Fourier transform infrared (FTIR) spectra were recorded as a KBr disk on a Galaxy series 5000 Fourier transform infrared spectrometer.

Synthesis of NHNPs

NHNPs were synthesized using a simple coordination precipitation procedure as in a previous report [33]. Briefly, by adding concentrated ammonia (28 wt%) to a nickel nitrate solution (1 M), a deep blue-colored nickel hexamine complex solution was formed. The solution was added into a given amount of distilled water, and the reaction was carried out under magnetic stirring for 1 h at 70 °C. Finally, light green sediments were formed. The precipitate was separated by centrifugation, rinsed with distilled water and ethanol three times, respectively, to remove the adsorbed ions, and then dried in a vacuum oven at 80 °C for 12 h to form a green powder of NHNPs. The FTIR spectrum was assigned for NHNPs (not shown). The sharp peak at 3650 cm^{-1} is assigned to the O-H stretching vibrational mode of nonhydrogen-bonded hydroxyl groups in nickel hydroxide. The peak at 519 cm^{-1} is attributed to the inplane deformation vibration of water (νOH) and the shoulder absorption at 490 cm^{-1} to the stretching vibration of Ni-OH (νNi-OH).

Synthesis of MCM-41

MCM-41 was synthesized through the self-assembly of inorganic silica precursor in our laboratory. A typical MCM-41 preparation procedure is described as follows: 13.0 g of hexadecyltrimethylammonium bromide was dissolved in 170 mL of deionized water, and then, 163.7 g of the aqueous ammonia and 131.5 g of ethanol were added to the surfactant solution. The solution was stirred for 15 min, and afterward, 24.8 g of tetraethyl orthosilicate (TEOS) was added. After 2 h of vigorous stirring with a mechanical stirrer at 1500 rpm and filtration, the white precipitate was successfully washed with plenty of deionized water and dried at 60 °C for 24 h. Before using MCM-41, a part of the MCM-41 sample was calcined under oxygen atmosphere by applying a heating ramp of 1 °C per min up to 600 °C and then kept at this temperature for 6 h [34]. The FTIR spectrum was assigned for MCM-41 (not shown). The band at 3434 cm^{-1} is assigned to the silanol groups linked to the molecular water via hydrogen bonds with internal Si-OH groups. The band at 1631 cm^{-1} is contributed by the absorbed molecular water. Other bands are as follows: 1083 cm^{-1} for Si-O-Si asymmetry stretching vibration, 812 cm^{-1} for Si-O-Si symmetry stretching vibration, and 464 cm^{-1} for Si-O-Si bending vibration.

Preparation of the modified electrode

The mixture of 5 % NHNPs, 10 % MCM-41, and 85 % MWCNTs was obtained as the optimum values for the fabrication of the sensor. Prior to modification, the GCE (3 mm diameter, Metrohm) was first polished with 0.3 and 0.05 μm aluminum slurry and rinsed thoroughly with triply distilled water. It was then cleaned by sonication for 5 min, first in ethanol and then distilled water, and then dried under a nitrogen gas flow. A stock solution of MWCNTs-NHNPs-MCM-41 in dimethylformamide (DMF) was prepared by dispersing 1.70 mg MWCNTs, 0.10 mg NHNPs, and 0.20 mg MCM-41 (85 %:5 %:10 % *w*/*w*) in 2 mL DMF using an ultrasonic bath until a homogeneous suspension solution resulted. After that, MWCNTs-NHNPs-MCM-41/GCE was prepared by coating the electrode surface with 20 μL of the stock solution. The electrode was then dried at room temperature overnight to obtain the modified electrode. This fabricated MWCNTs-NHNPs-MCM-41/GCE was placed in the electrochemical cell containing 0.1 M PBS, and 20 cycles in the potential windows of 0.0 to 1.0 V were performed using the CV method to obtain stable responses.

General procedure

Each sample solution (10 mL) containing appropriate amounts of DA, PRX, and CEF in 0.1 M PBS at pH 5 was transferred into the voltammetric cell. Calibration curves were obtained by plotting the anodic peak currents of DA, PRX,

and CEF against the corresponding concentrations. After each measurement, the MWCNTs-NHNPs-MCM-41/GCE was regenerated by thoroughly washing the electrode with triply distilled water and then 2 % sodium hydroxide solution to remove all adsorbate from the electrode surface. The electrode was finally rinsed carefully with distilled water to provide a clean and fresh surface for the next experiments. EIS was performed in a solution containing 5 mM of each of $Fe(CN)_6^{3-}$ and $Fe(CN)_6^{4-}$ and 0.1 M KCl with the frequency swept from 10^5 to 0.01 Hz at the condition potential of 0.22 V. All experiments were carried out under open circuit conditions. During accumulation of the analytes, the solution was under stirring.

Results and discussion

Effect of the composition of MWCNTs, NHNPs, and MCM-41

The effect of the composition of MWCNTs, NHNPs, and MCM-41 on the performance of the modified GCE was tested using cyclic voltammetry method (not shown). The ratio of NHNPs and MCM-41 influences the sensitivity of the sensor. It was found that as the ratio of NHNPs increased from 2 to 5 %, the response of the electrode improved, and when the ratio was more than 5 %, the response decreased with a larger background current. Further experiments showed that as the ratio of MCM-41 increased from 2 to 10 %, the response of the electrode improved, and when the ratio was more than 10 %, the response decreased with a larger background current, which led to poor electrochemical measurements for DA, PRX, and CEF.

Characterization of the MWCNTs-NHNPs-MCM-41 composite

We have previously reported the characterization of NHNPs using XRD and TEM [35]. Figure 1a shows the SEM image of the MWCNTs-NHNPs. A platelet-like nanostructure is shown with a dimension in the range of 50–100 nm. Figure 1b shows a typical image of the MWNTs-MCM-41. The particle sizes of MCM-41 are between 200 and 400 nm. It can be seen that the MCM-41 is well covered with MWCNTs. In addition to the well-distributed small particles, large agglomerated particles are also observed. The SEM image of the MWCNTs-NHNPs-MCM-41 (Fig. 1c) shows that the MCM-41 surface was mostly covered with MWCNTs and NHNPs. The porosity of MCM-41 leads to an increase in the surface area of the composite; therefore, a higher peak current could be obtained on the modified electrode with this composite. Energy-dispersive X-ray (EDX) analysis of the MWCNTs-NHNPs-MCM-41 composite shows the presence of Si, Ni, O, and C (Fig. 1d). A high percentage of Si could be due to the Si base of the plate (pyrolyzed photoresist film—PPF). The presence of Ni and O peaks accompanied by Si content confirms the successful modification of MWCNT.

EIS can provide some information including the electrode impedance, the capacity of the electrical double layer, and the

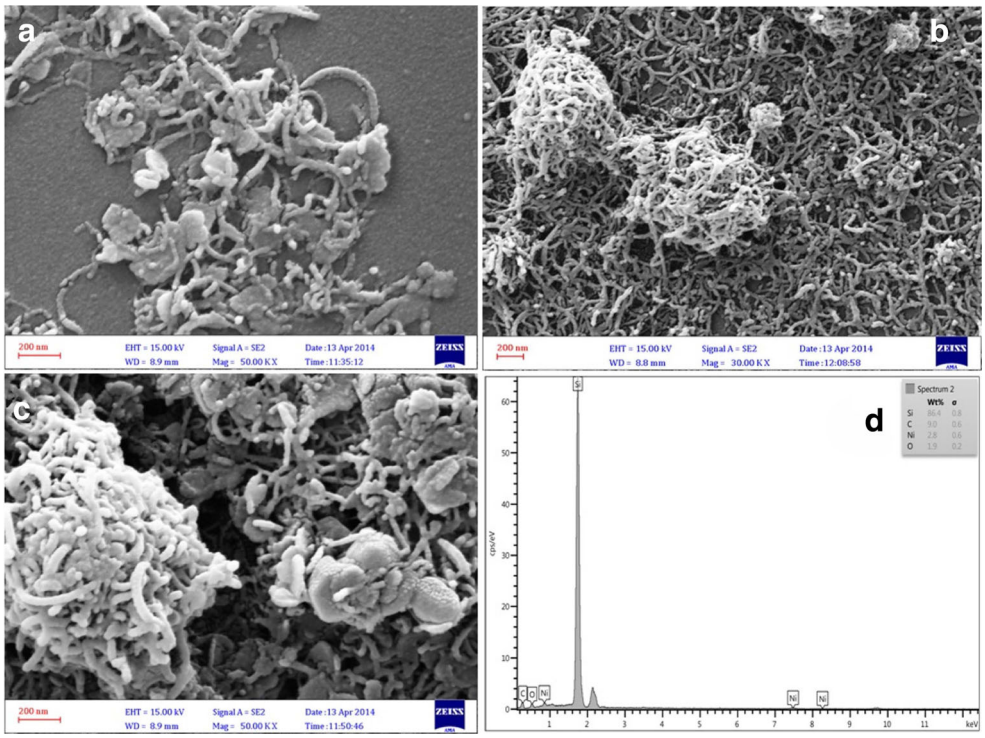

Fig. 1 SEM micrographs of the samples: **a** MWCNTs-NHNPs, **b** MWCNTs-MCM-41, and **c** MWCNTs-NHNPs-MCM-41. **d** SEM-EDX spectrum of MWCNTs-NHNPs-MCM-41

surface electron transfer resistance (Rct) of the electrode surface as a result of the modification process. Figure 2 shows the Nyquist plots (−Z″ vs. Z′) for MWCNTs-NHNPs-MCM-41/GCE (Fig. 2A), MWCNTs-NHNPs/GCE (Fig. 2B), and GCE (Fig. 2C) electrodes obtained when the electrodes were immersed in a 0.1-M KCl solution containing 5 mM of mixture of $K_3[Fe(CN)_6]$ and $K_4[Fe(CN)_6]$. In the Nyquist diagram, the semicircle diameter of EIS is equal to Rct. The results showed that the diameters of the semicircle for the MWCNTs-NHNPs-MCM-41/GCE and MWCNTs-NHNPs/GCE were 0.209 and 0.221 kΩ, respectively, which are smaller than that of the unmodified GCE (3.014 kΩ). The results suggest that the MWCNTs-NHNPs-MCM-41 and MWCNTs-NHNPs composite modification of the electrode provides a significant acceleration for $[Fe(CN)_6]^{3-/4-}$ redox reaction on the electrode surface.

Electrochemical behavior of DA, PRX, and CEF on MWCNTs-NHNPs-MCM-41/GCE

Figure 3 shows the differential pulse voltammograms of a solution of 70 μM of DA, 60 μM of PRX, and 160 μM of CEF in PBS (pH=5) at bare and modified GC electrode. The differential pulse voltammograms were recorded by applying positive-going potential from 0 to 0.8 V. The voltammograms showed anodic peaks around 0.13, 0.40, and 0.62 V corresponding to the DA, PRX, and CEF compounds, respectively. The corresponding peak heights were proportional to their concentrations in the solutions. As can be seen (curve a in Fig. 3), small oxidation peak potentials for DA, PRX, and CEF at bare GCE were obtained. The MWCNT-modified GCE significantly enhanced the anodic peak currents compared with the bare GCE (curve b in Fig. 3), which can be related to the high surface area and electrocatalytic behavior of MWCNTs. In addition, the MCM-41-modified GCE showed significant improvement in the anodic peak currents compared with the bare GCE (curve c in Fig. 3), which can be related to the high surface area of MCM-41. It can also be seen that the peak current of DA, PRX, and CEF increases further at the MWCNTs-NHNPs/GCE (curve d in Fig. 3). In addition, the peaks shifted to a lower potential which confirms the electrocatalytic behavior of NHNPs. DA, PRX, and CEF showed the highest oxidation peak at the MWCNTs-NHNPs-MCM-41/GCE without a significant potential shift with respect to curve d which could be due to a higher surface provided by MCM-41 in the composite (curve e in Fig. 3). The enhancement in peak currents and the lowering of overpotentials

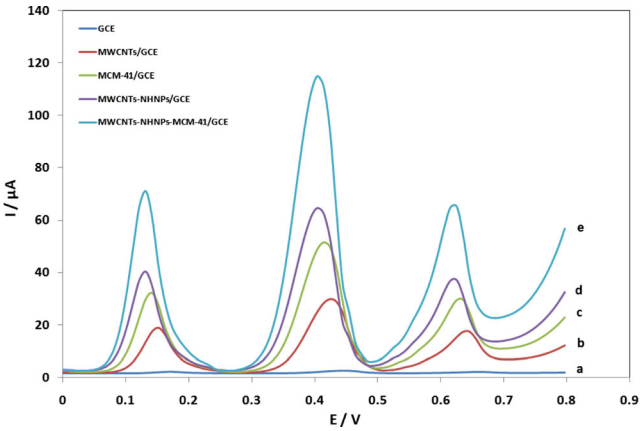

Fig. 3 Differential pulse voltammograms of 70 μM DA, 60 μM PRX, and 160 μM CEF at *a* GCE, *b* MWCNTs/GCE, *c* MCM-41/GCE, *d* MWCNTs-NHNPs/GCE, and *e* MWCNTs-NHNPs-MCM-41/GCE in 0.1 M phosphate buffer solution (pH 5). Other conditions: open circuit, t_{acc}=40 s, pulse amplitude=50 mV, scan rate=10 mV s^{-1}, interval time 0.5 s, modulation time=0.2 s, and step potential=5 mV

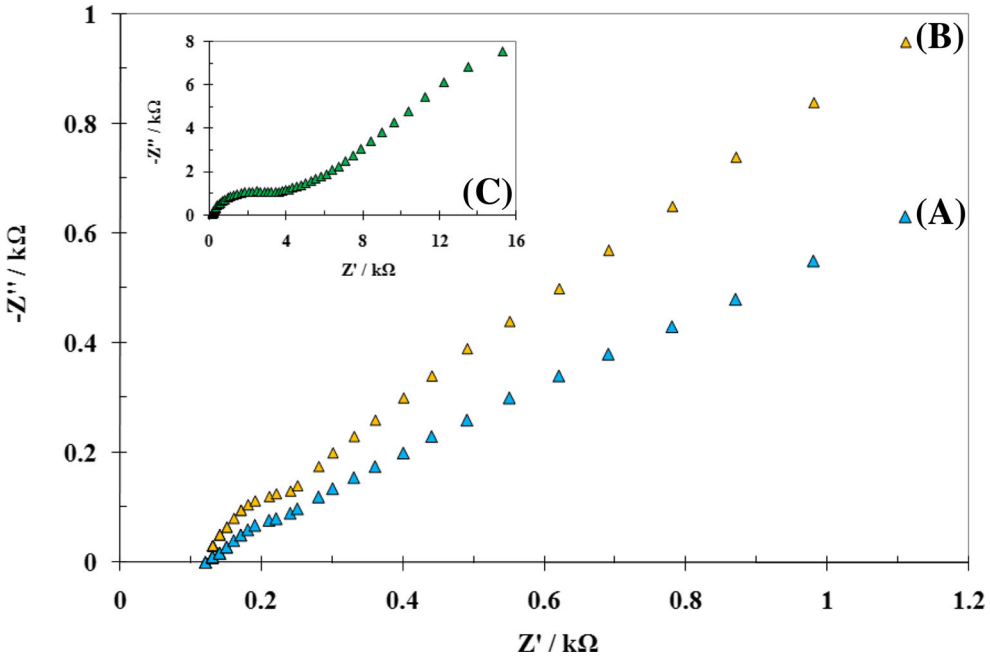

Fig. 2 Nyquist plots for MWCNTs-NHNPs-MCM-41/GCE (*A*), MWCNTs-NHNPs/GCE (*B*), and GCE (*C*) electrodes obtained when the electrodes were immersed into solutions of 5 mM $K_3[Fe(CN)_6]/K_4[Fe(CN)_6]$ and 0.1 M KCl solution

between DA, PRX, and CEF are clear lines of evidence of the synergistic electrocatalytic effects and the high surface area of MWCNTs-NHNPs-MCM-41 composite toward oxidations of the DA, PRX, and CEF.

Effects of the scan rate

The effect of potential scan rate on the oxidation responses of DA, PRX, and CEF over the range of 10–250 mV s^{-1} scan rate was investigated (not shown). The linear relationships between the anodic peak currents and scan rates were observed for DA in the range of 10–110 mV s^{-1}, PRX in the range of 10–100 mV s^{-1}, and CEF in the range of 10–110 mV s^{-1} and shown as follows:

$$\begin{aligned} \text{Ipa}\ (\mu\text{A}) &= 1.027\nu(\text{mV s}^{-1}) + 11.56 \quad (R^2 = 0.998) \quad \text{DA} \\ \text{Ipa}\ (\mu\text{A}) &= 1.841\nu(\text{mV s}^{-1}) + 13.34 \quad (R^2 = 0.993) \quad \text{PRX} \\ \text{Ipa}\ (\mu\text{A}) &= 0.325\nu(\text{mV s}^{-1}) + 6.33 \quad (R^2 = 0.989) \quad \text{CEF} \end{aligned}$$

The linear relationship between peak currents and scan rates suggests that the oxidation reactions of all three compounds at MWCNTs-NHNPs-MCM-41/GCE are adsorption-controlled processes at such scan rates.

Optimization of experimental variables

Effects of solution pH

The effect of solution pH on the electrochemical response of the MWCNTs-NHNPs-MCM-41/GCE toward DA, PRX, and CEF in the simultaneous determination of 70 μM DA, 60 μM PRX, and 160 μM CEF was investigated using the DPV method (Fig. 4). From Fig. 4 (inset A), it can be found that the peak currents for the three compounds were suitable at pH=5. Therefore, the pH value of 5 was chosen as the optimum solution pH for further experiments.

Figure 4 (inset B) shows the relationship between the oxidation peak potential of DA, PRX, and CEF with pH. It was found that by the variation of pH, the corresponding oxidation peak potentials for DA, PRX, and CEF vary linearly with pH as follows:

$$\begin{aligned} \text{Epa versus Ag/AgCl(mV)} &= 982–60\text{pH} \quad (R^2 = 0.9972) \quad \text{DA} \\ \text{Epa versus Ag/AgCl(mV)} &= 706–50\ \text{pH} \quad (R^2 = 0.9981) \quad \text{PRX} \\ \text{Epa versus Ag/AgCl(mV)} &= 469–55\ \text{pH} \quad (R^2 = 0.9899) \quad \text{CEF} \end{aligned}$$

The slopes of the variations of Ep as a function of solution pH are close to the Nernstian slope of 59, which suggests an equal number of electrons and protons involved in the electrochemical oxidations of DA, PRX, and CEF.

Effects of accumulation time

The effect of accumulation time on the electrochemical response of the MWCNTs-NHNPs-MCM-41/GCE toward DA, PRX, and CEF in the simultaneous determination of 40 μM DA, 30 μM PRX, and 90 μM CEF was investigated using the DPV method in PBS (pH=5) (not shown). Initially, regarding the peak current for DA, PRX, and CEF, the corresponding oxidation peak current increases up to 40 s and then levels off.

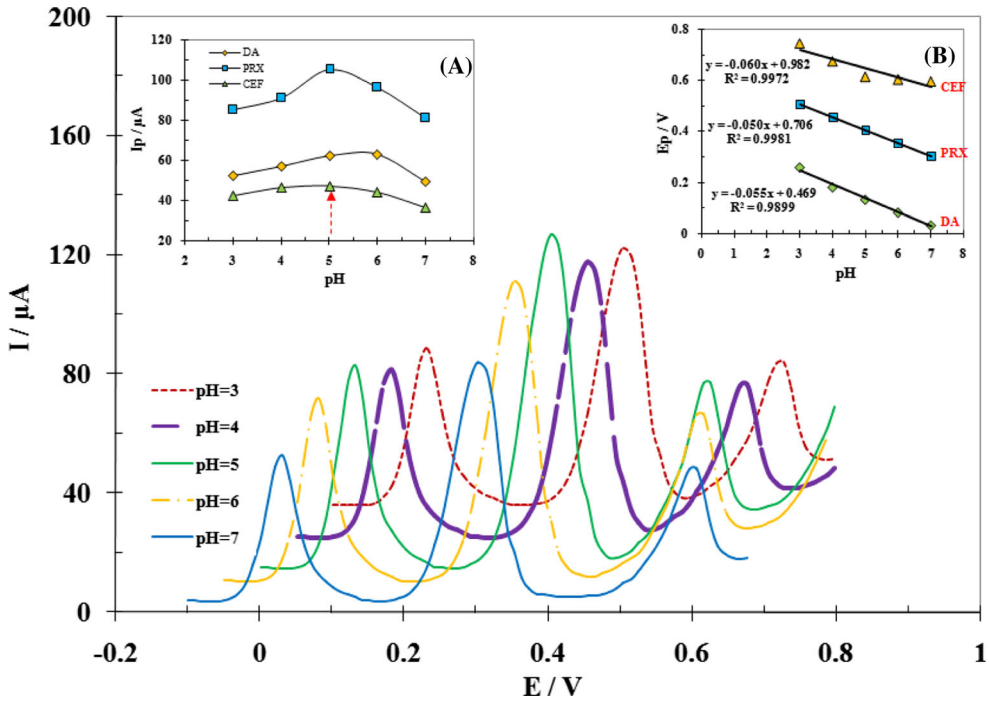

Fig. 4 Effect of pH on the differential pulse voltammograms of 40 μM DA, 60 μM PRX and 80 μM CEF compounds at MWCNTs-NHNPs-MCM-41/GCE in 0.1 M phosphate buffer. Insets: **a** Plot of anodic peak currents (Ipa) as a function of pH of buffer solutions. **b** Plot of peak potentials (Ep) as a function of pH of buffer solutions

Therefore, the accumulation time of 40 s was chosen as the optimum time for further experiments.

Linear dynamic range and detection limit of the method

The electrochemical responses of the simultaneous additions of solutions of DA, PRX, and CEF in a 0.1-M PBS pH 5 using MWCNTs-NHNPs-MCM-41/GCE are depicted in Fig. 5. The figure shows differential pulse voltammograms and the corresponding calibration curves obtained for various concentrations of DA, PRX, and CEF at MWCNTs-NHNPs-MCM-41/GCE. For DA, a linear dynamic range from 0.2 to 85 μM with a calibration equation of Ip (μA)=1.0053*c* (μM)+0.7271 (R^2=0.9989) and a detection limit of 0.07 μM (S/N=3) were obtained. For PRX, a linear dynamic range from 0.1 to 70 μM with a calibration equation of Ip (μA)=2.020*c* (μM)+0.6336 (R^2=0.9992) and a detection limit of 0.04 μM (S/N=3) were obtained. For CEF, a linear relationship was found over the range of 0.1 to 200 μM with a calibration equation of Ip (μA)=0.2971*c* (μM)+0.4074 (R^2=0.9992) and a detection limit of 0.05 μM. The results showed that these linear ranges were kept in mixture solutions of DA, PRX, and CEF, revealing the high efficiency of the fabricated modified electrode for simultaneous determinations of these compounds in mixed pharmaceutical samples.

Figure 6 displays a chronoamperogram of the response of a rotated modified electrode (3000 rpm) following the successive injection of DA, PRX, and CEF at an applied potential of 0.7 V in PBS (pH=5). For DA, the linear dynamic range was from 1 to 186 μM, with a calibration equation of Ip (μA)=1.1316*c* (μM)+4.6148 (R^2=0.9979), and a detection limit of 0.3 μM (S/N=3) was obtained. For PRX, the linear dynamic range was from 0.5 to 185 μM, with a calibration equation of Ip (μA)=1.4962*c* (μM)+4.2047 (R^2=0.9978), and a detection limit of 0.1 μM (S/N=3) was obtained. For CEF, the linear relationship was in the range of 0.5 to 290 μM with a calibration equation of Ip (μA)=0.4923*c* (μM)+1.9401 (R^2=0.9989), and a detection limit of 0.2 μM (S/N=3) was obtained.

Repeatability and long-term stability of the electrode

The repeatability of the modified electrode was studied, and relative standard deviations (RSD) of 2.14, 1.97, and 1.63 % for ten consecutive determinations of 40 μM DA, 60 μM PRX, and 80 μM CEF were obtained, respectively.

The proposed modified electrode has a further attraction of good long-term stability. This was tested by measuring the decrease in voltammetric current during repetitive DPV measurements of DA, PRX, and CEF solutions with MWCNTs-NHNPs-MCM-41/GCE stored in a solution or air for a certain period of time. For example, in the determination of 40 μM DA, 60 μM PRX, and 80 μM CEF in 0.1 M PBS (pH=5), when the modified electrode was stored in a buffer solution and then subjected to an experiment every 60 min, after 36 h, there were decreases of less than 8.8, 6.2, and 8.9 % in the voltammetric currents of DA, PRX, and CEF, respectively. When the electrode was stored in the atmosphere for 7 days, the oxidation peak current of DA, PRX, and CEF in the solution was reduced less than 8.1, 7.4, and 6.7 %, respectively. The results confirmed the high stability of the proposed modified electrode.

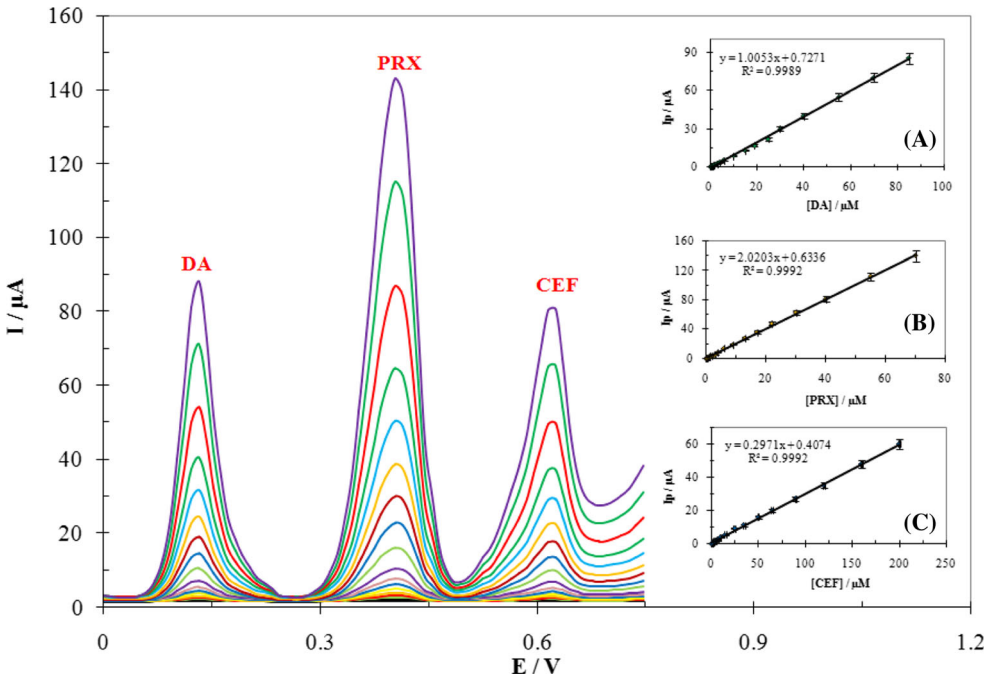

Fig. 5 Differential pulse voltammograms for different concentrations of DA, PRX, and CEF mixtures. *Insets*: *A* plot of peak currents as a function of DA concentration, *B* plot of peak currents as a function of PRX concentration, and *C* plot of the peak currents as a function of CEF concentration

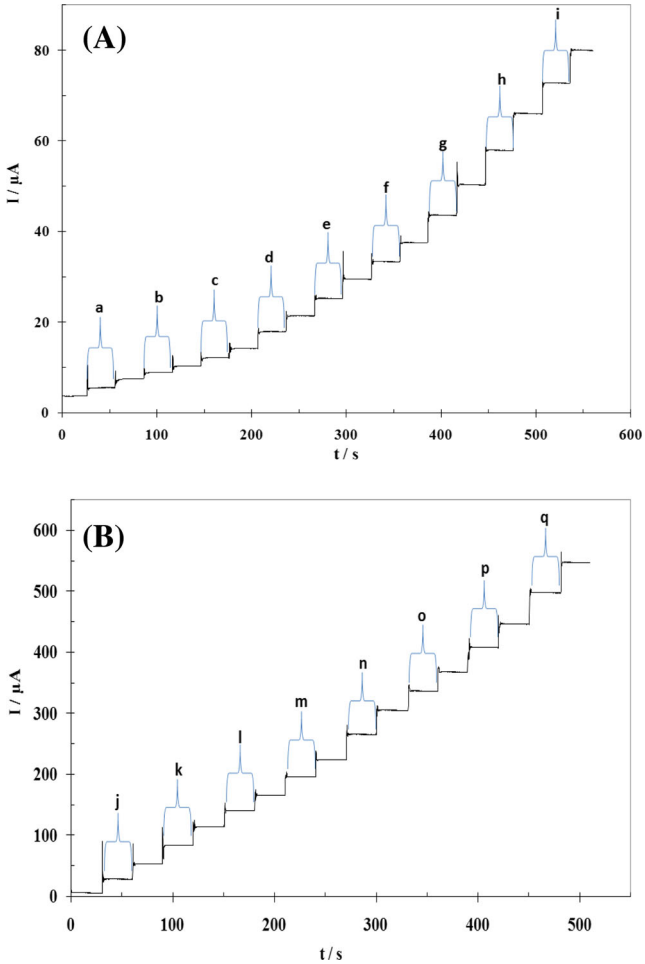

Fig. 6 Hydrodynamic chronoamperometric response at rotating MWCNTs-NHNPs-MCM-41/GCE (rotating speed 3000 rpm) held at 0.7 V in PBS (pH=5) for successive additions in micromolars of *a* 1 DA, *b* 0.5 PRX, *c* 0.5 CEF, *d* 2 DA, *e* 2 PRX, *f* 7 CEF, *g* 5 DA, *h* 5 PRX, *i* 15 CEF, *j* 20 DA, *k* 20 PRX, *l* 50 CEF, *m* 25 DA, *n* 25 PRX, *o* 70 CEF, *p* 40 DA, and *q* 40 PRX

Interference studies

The influences of common interfering species in the presence of 40 μM DA, 60 μM PRX, and 80 μM CEF under optimum conditions were investigated. The results confirmed that interfering species did not significantly influence the height of the peak currents for DA, PRX, and CEF. The tolerance limits (defined as the concentrations which give an error of ≤10 %) for some of the most common interfering agents are shown in Table 2. The results show that the proposed method is free from interferences of the most common interfering agents.

Table 2 Maximum tolerable concentration of interfering species

Interfering species	DA C_{int} (μM)	PRX C_{int} (μM)	CEF C_{int} (μM)
Aspartic acid	800	1100	900
L-Glutamic acid	1200	1300	1400
L-Alanine	1200	2200	1300
L-Histidine	1000	1400	1000
Ascorbic acid	400	1200	1100
Uric acid	150	500	400
Tryptophan	900	1000	500
Tyrosine	1600	1700	800

C_{int} refers to interfering compound concentration

Table 3 Determination of DA, PRX, and CEF in human serum with MWCNTs-NHNPs-MCM-41/GCE

Analyte	Added (μM)	Found[a] (μM)	RSD (%)	Recovery (%)
DA	0	0	–	–
	10.0	10.5	4.5	105.0
	30.0	31.1	3	103.7
PRX	0	0	–	–
	20.0	20.5	4.2	102.5
	30.0	29.3	2.9	97.7
CEF	0	0	–	–
	20.0	19.2	2.9	96.0
	40.0	39.5	2.2	98.8

[a] Average of five determinations at optimum conditions

Analytical applications

The applicability of a MWCNTs-NHNPs-MCM-41/GC electrode to the determination of DA, PRX, and CEF in human serum and human urine was examined. Differential pulse voltammograms were obtained by spiking prepared real solutions with appropriate samples and using MWCNTs-NHNPs-MCM-41/GCE at optimum conditions. Concentrations were measured by applying the calibration plot using the standard addition method. The results are shown in Tables 3 and 4. The good recoveries indicate that both the accuracy and repeatability of our proposed method are superior. From the above experimental results, it is very clear that this method has great potential for the determination of trace

Table 4 Determination of DA, PRX, and CEF in human urine with MWCNTs-NHNPs-MCM-41/GCE

Analyte	Added (μM)	Found[a] (μM)	RSD (%)	Recovery (%)
DA	0	0	–	–
	10.0	9.9	3.4	99.0
	30.0	30.7	2.8	102.3
PRX	0	0	–	–
	20.0	19.8	2.9	99.0
	30.0	29.0	3.1	96.7
CEF	0	0	–	–
	40.0	39.3	3.5	98.2
	50.0	50.3	2.6	100.6

[a] Average of five determinations at optimum conditions

amounts of these compounds in biological systems or pharmaceutical preparations.

Conclusions

In this report, the new application of a sensor based on MWCNTs-NHNPs-MCM-41 is introduced. The combination of NHNPs, MWCNTs, and MCM-41 leads to an excellent electrocatalytic performance for the simultaneous determination of DA, PRX, and CEF. The electrode also shows high stability in repetitive experiments. The interfering study of some species showed no significant interference with the determination of DA, PRX, and CEF. The application of the proposed sensor for the determination of DA, PRX, and CEF in some real samples gave satisfactory results, without the necessity of sample pretreatments or time-consuming extractions. The high speed, reproducibility, high stability, wide linear dynamic range, and low detection limit suggest that the proposed sensor is an attractive candidate for practical applications.

Acknowledgments The authors gratefully acknowledge the Research Council of Arak University for providing financial support (No. 92.9829) for this work.

References

1. Che G, Lakshmi BB, Fisher ER, Martin CR (1998) Carbon nanotubule membranes for electrochemical energy storage and production. Nature 393:346–349
2. Roucoux A, Schulz J, Patin H (2002) Reduced transition metal colloids: a novel family of reusable catalysts? Chem Rev 102: 3757–3778
3. Yu JG, Zhao XH, Yang H, Chen XH, Yang Q, Yu LY, Jiang JH, Chen XQ (2014) Aqueous adsorption and removal of organic contaminants by carbon nanotubes. Sci Total Environ 482:241–251
4. Fu GR, Hu ZA, Xie LJ, Jin XQ, Xie YL, Wang YX, Zhang ZY, Yang YY, Wu HY (2009) Electrodeposition of nickel hydroxide films on nickel foil and its electro-chemical performances for supercapacitor. Int J Electrochem Sci 4:1052–1062
5. Babaei A, Sohrabi M, Afrasiabi M (2012) A sensitive simultaneous determination of epinephrine and piroxicam using a glassy carbon electrode modified with a nickel hydroxide nanoparticles/multiwalled carbon nanotubes composite. Electroanalysis 24:2387–2394
6. Li XL, Liu JF, Li YD (2003) Low-temperature conversion synthesis of $M(OH)_2$ (M = Ni, Co, Fe) nanoflakes and nanorods. Mater Chem Phys 80:222–227
7. Kresge CT, Leonowicz ME, Roth WJ, Vartuli JC, Beck JS (1992) Ordered mesoporous molecular sieves synthesized by a liquid-crystal template mechanism. Nature 359:710–712
8. Sayari A (1996) Catalysis by crystalline mesoporous molecular sieves. Chem Mater 8:1840–1852
9. Jiang YX, Song WB, Liu Y, Wei B, Cao XC, Xu HD (2000) Electrochemical characterization of the host-guest nanocomposite material MCM-41-based iron and ruthenium complexes with bipyridine and phenanthroline. Mater Chem Phys 62:109–114
10. Rathousky J, Zukai A, Franke O, Schulz-Ekloff G (1995) Adsorption on MCM-41 mesoporous molecular sieves. Part 2. Cyclopentane isotherms and their temperature dependence. J Chem Soc Faraday Trans 91:937–940
11. Li J, Huang M, Liu X, Wei H, Xu Y, Xu G, Wang E (2007) Enhanced electrochemiluminescence sensor from tris(2,2′-bipyridyl)ruthenium(II) incorporated into MCM-41 and an ionic liquid-based carbon paste electrode. Analyst 132:687–691
12. Guo H, He N, Ge S, Yang D, Zhang J (2005) MCM-41 mesoporous material modified carbon paste electrode for the determination of cardiac troponin I by anodic stripping voltammetry. Talanta 68:61–66
13. Wang F, Yang J, Wu K (2009) Mesoporous silica-based electrochemical sensor for sensitive determination of environmental hormone bisphenol A. Anal Chim Acta 638:23
14. Damier P, Hirsch EC, Agid Y, Graybiel AM (1999) The substantia nigra of the human brain II. Patterns of loss of dopamine-containing neurons in Parkinson's disease. Brain 122:1437–1448
15. Wightman RM, May LJ, Michael AC (1988) Detection of dopamine dynamics in the brain. Anal Chem 60:769A–779A
16. Gilman A, Goodman L, Goodman GS (2005) The pharmacological basis of therapeutics. McGraw-Hill Professional, New York
17. Escandar GM (1999) Spectrofluorimetric determination of piroxicam in the presence and absence of β-cyclodextrin. Analyst 124:587–591
18. Puthli SP, Vavia PR (2000) Stability indicating HPTLC determination of piroxicam. J Pharm Biomed Anal 22:673–677
19. Gonzalez-Hernandez R, Nuevas-Paz L, Soto-Mulet L, Lopez-Lopez M, Hoogmartens J (2001) Reversed phase high performance liquid chromatographic determination of cefixime in bulk drugs. J Liq Chromatogr Relat Technol 24:2315–2324
20. Eric-Jovanovic S, Agbaba D, Zivanov-Stakic D, Vladimirov S (1998) HPTLC determination of ceftriaxone, cefixime and cefotaxime in dosage forms. J Pharm Biomed Anal 18:893–898
21. Bebawy LI, El Kelani K, Fattah LA (2003) Fluorimetric determination of some antibiotics in raw material and dosage forms through ternary complex formation with terbium (Tb3+). J Pharm Biomed Anal 32:1219–1225
22. Ensafi AA, Allafchian AR (2013) Multiwall carbon nanotubes decorated with NiFe2O4 magnetic nanoparticles, a new catalyst for voltammetric determination of cefixime. Colloids Surf B 102:687–693
23. Afkhami A, Soltani-Felehgari F, Madrakian T (2013) Gold nanoparticles modified carbon paste electrode as an efficient electrochemical sensor for rapid and sensitive determination of cefixime in urine and pharmaceutical samples. Electrochim Acta 103:125–133
24. Katzung BG (2004) Basic & clinical pharmacology. McGraw-Hill Medical, New York
25. Huang J, Liu Y, Hou H, You T (2008) Simultaneous electrochemical determination of dopamine, uric acid and ascorbic acid using palladium nanoparticle-loaded carbon nanofibers modified electrode. Biosens Bioelectron 24:632–637
26. Karimi Shervedani R, Alinajafi-Najafabadi HA (2011) Electrochemical determination of dopamine on a glassy carbon electrode modified by using nanostructure ruthenium oxide hexacyanoferrate/ruthenium hexacyanoferrate thin film. Int J Electrochem 2011:1–11
27. Keeley GP, McEvoy N, Nolan H, Kumar S, Rezvani E, Holzinger M, Cosniera S, Duesberg GS (2012) Simultaneous electrochemical determination of dopamine and paracetamol based on thin pyrolytic carbon films. Anal Methods 4:2048–2053
28. Guo Z, Seol ML, Kim MS, Ahn JH, Choi YK, Liu JH, Huang XJ (2013) Sensitive and selective electrochemical detection of dopamine using an electrode modified with carboxylated carbonaceous spheres. Analyst 138:2683–2690

29. Zhuang Z, Li J, Xu R, Xiao D (2011) Electrochemical detection of dopamine in the presence of ascorbic acid using overoxidized polypyrrole/graphene modified electrodes. Int J Electrochem Sci 6: 2149–2161
30. Shahrokhian S, Jokar E, Ghalkhani M (2010) Electrochemical determination of piroxicam on the surface of pyrolytic graphite electrode modified with a film of carbon nanoparticle-chitosan. Microchim Acta 170:141–146
31. Abbaspour A, Mirzajani R (2007) Electrochemical monitoring of piroxicam in different pharmaceutical forms with multi-walled carbon nanotubes paste electrode. J Pharm Biomed Anal 44:41–48
32. Reddy TM, Sreedhar M, Jayarama Reddy S (2003) Voltammetric behavior of cefixime and cefpodoxime proxetil and determination in pharmaceutical formulations and urine. J Pharm Biomed Anal 31: 811–818
33. Xiao-Yan G, Jian-cheng D (2007) Preparation and electrochemical performance of nano-scale nickel hydroxide with different shapes. Mater Lett 61:621–625
34. Martins L, Cardoso D (2007) Influence of surfactant chain length on basic catalytic properties of Si-MCM-41. Microporous Mesoporous Mater 106:8–16
35. Babaei A, Taheri AR (2013) Nafion/Ni$(OH)_2$ nanoparticles-carbon nanotube composite modified glassy carbon electrode as a sensor for simultaneous determination of dopamine and serotonin in the presence of ascorbic acid. Sensors Actuators B 176:543–551